doi: 10.18323/2782-4039-2023-4-66-9

Structure and micromechanical properties of SHS composites with a copper matrix: peculiarities of formation

Nataliya B. Pugacheva[1], Doctor of Sciences (Engineering), Associate Professor, chief researcher
Tatyana M. Bykova*[2], PhD (Engineering), senior researcher
Ekaterina I. Senaeva[3], junior researcher
Institute of Engineering Science of the Ural Branch of RAS, Yekaterinburg (Russia)

***E-mail: nat@imach.uran.ru, tatiana_8801@mail.ru**

[1]ORCID: https://orcid.org/0000-0001-8015-8120
[2]ORCID: https://orcid.org/0000-0002-8888-6410
[3]ORCID: https://orcid.org/0000-0001-8625-2310

Received 22.06.2023 *Accepted 19.10.2023*

Abstract: Self-propagating high-temperature synthesis (SHS) is one of the promising methods for producing strong and wear-resistant composites. The use of copper as a matrix due to the unique combination of electrical and thermal conductivity is of particular interest. Monolithic SHS composites of the Cu–Ti–C–B and Cu–Ti–C systems are currently little studied. The information on the phase composition of such composites is contradictory, and data on micromechanical properties is practically absent. The paper presents the results of a comparative analysis of the structure and micromechanical properties of composites of the Cu–Ti–C and Cu–Ti–C–B systems. It is found that the matrix of both composites is a copper-based solid solution supersaturated with titanium, in which nanosized Cu_4Ti intermetallic compound particles precipitate upon cooling. TiC particles (Cu–Ti–C composite) and TiC and TiB_2 particles (Cu–Ti–C–B composite) are the strengthening phases resulting from SHS. In the Cu–Ti–C–B composite, the original particles of unreacted B_4C boron carbide were preserved, the microhardness of which was 3680 *HV* 0.1. The most ductile structural constituent in the Cu–Ti–B system composite is the Cu+Cu_4Ti mechanical mixture, due to which further plastic deformation is possible to obtain parts of a given shape. During the study of micromechanical properties, the maximum strength indicators of H_{IT}, *HV*, W_e, R_e, H_{IT}/E^* were recorded in the Cu–Ti–C–B system composite, which allows expecting high wear resistance of products made of it.

Keywords: self-propagating high-temperature synthesis; monolithic SHS composites; copper matrix; structural constituents; strengthening phases; intermetallides; titanium carbide; titanium diboride; micromechanical properties; hardness.

Acknowledgments: The research was supported by the Russian Science Foundation grant No. 22-29-00188 "The Development of Scientific and Technological Foundations for the Formation of Monolithic SHS Composites of the Cu–Ti–C–B System with Specified Functional Properties", https://rscf.ru/project/22-29-00188/.

The work was performed on the equipment of the "Plastometria" Core Facility Center of the Federal State Budgetary Institution of Science Institute of Engineering Science, Ural Branch of the Russian Academy of Sciences.

The paper was prepared on the reports of the participants of the XI International School of Physical Materials Science (SPM-2023), Togliatti, September 11–15, 2023.

For citation: Pugacheva N.B., Bykova T.M., Senaeva E.I. Structure and micromechanical properties of SHS composites with a copper matrix: peculiarities of formation. *Frontier Materials & Technologies*, 2023, no. 4, pp. 99–108. DOI: 10.18323/2782-4039-2023-4-66-9.

INTRODUCTION

The method of self-propagating high-temperature synthesis (SHS) is widely recognised in the field of creating new powder materials [1–3]. Currently, this process is being studied in 47 countries around the world. The SHS process is based on carrying out exothermic chemical reactions of interaction of initial reagents in the form of combustion, where the target combustion product is solid chemical compounds (carbides, nitrides, borides, oxides, etc.) and materials based on them [4]. The main reagents in SHS processes are powders of metals and non-metals, and the final product is powders, sintered bulk materials or coatings [5–7].

The advantages of SHS technology include a significant reduction in energy costs for heating to high temperatures, as the heat generated by the combustion reaction works, as well as the use of simple, small-scale equipment, and the implementation of high process speeds [8–10]. Currently, about 100 varieties of SHS technology have been created, which allow synthesising over 1000 substances and materials, applying coatings, and welding parts. In Russia, six types of SHS technologies are common: reactor powder, sintering, power compaction, casting and weld facing, welding, and vapour transport coatings [3; 8]. SHS technologies are widely used in mechanical engineering (abrasive, blade and stamp tools, high-temperature and wear-resistant parts), metallurgy (refractory products, weld facing, electrodes, ferroalloys, metal-supplying pipes), electrical engineering and electronics (ferrites, ferroelectric materials, insulators, heating elements, high-temperature superconductors), chemical industry (catalysts), medicine (implants made of shape memory alloys) [9]. The SHS process is also very promising for the production of nanomaterials: nanosized powders, fibres and films, as well as nanostructured compact materials [10].

SHS is a rather complex physical and chemical process; its behaviour depends on many factors: the reaction heat,

the composition and structure of the initial mixture of powders, the size of their particles, density, size and temperature of samples, the composition and pressure of the surrounding gas, etc. SHS is based on the exothermic reactions leading to heating of the initial mixture up to the melting point of the metal powders that form the composite matrix [3; 4]. After the SHS completion, the produced composite is cooled, and, as a result, phase transformations are possible in the metal matrix that largely determine the composite properties. Until now, research has been focused mainly on studying the theory of combustion and synthesis processes, understanding their mechanisms, identifying the influence of various technological parameters on the composition, structure and properties of the resulting product, as well as developing the equipment for the SHS process implementation [3; 4]. The study of the structure and properties of the matrix is rather neglected. However, it is in it that significant changes occur both during the synthesis process and during subsequent thermal treatments [11–13]: during the combustion process, supersaturated solid solutions, non-equilibrium phases and intermediate products are formed, which upon subsequent heating, can decay and interact with each other, forming new phases.

Copper has a unique combination of electromagnetic and thermophysical properties [14]. Therefore, composites with a copper matrix are a very promising new material for structures requiring high electrical and thermal conductivity [15; 16]. The authors of works [14; 17] showed that severe plastic deformation of Cu/Mg composites, in combination with heat treatment allows obtaining unique properties due to a combination of high electrical conductivity and strength. Previous studies have demonstrated that composites of the Cu–Ti–C and Cu–Ti–C–B systems are characterised by high wear resistance [18; 19]. It has been found that abrasive wear of these composites occurs through plastic displacement of the cut material, which allows forming a surface with a high degree of roughness [19]. Moreover, copper and alloys based on it are quite easily deformed, which allows implementing deformation-thermal treatment of the composite to change its properties and give it a defined shape. Thus, in the work [20], temperatures and pressures were found at which it is possible to realise plastic deformation of the Cu–Ti–C–B SHS composite without destruction. In this regard, the study of composites of the Cu–Ti–C and Cu–Ti–C–B systems is of great practical interest.

The available information on the phase composition of SHS composites of the Cu–Ti–C and Cu–Ti–C–B systems is quite contradictory. Thus, the authors of [18] discovered, except for the particles of strengthening TiC phases formed as a result of the Cu–Ti–C composite SHS, a whole series of titanium cuprides of various compositions. The works [19; 20] show that in the copper matrix of Cu–Ti–C–B composites, nano-sized particles of only one intermetallic compound, Cu_4Ti, homogeneously precipitate. Moreover, previous studies [21] showed that when forming Cu–Ti–C–B system composites, it is possible to retain a small amount of B_4C particles, that do not have time to react with titanium [21]. In this regard, it is of interest to conduct a comparative analysis of the structure of Cu–Ti–C and Cu–Ti–C–B composites produced under the same conditions using the same Cu, Ti, and C powders, differing only in the addition of B_4C powder to the composition of the original mixtures.

The purpose of the work is to carry out a comparative analysis of the structure and micromechanical properties of SHS composites of the Cu–Ti–C and Cu–Ti–C–B systems.

METHODS

Monolithic composites of the Cu–Ti–C and Cu–Ti–C–B systems were produced using a technology described in detail previously in [22].

The initial powder mixture consists of thermoreactive and matrix components. Thermoreactive components (TRC) are powders of PTM-1 titanium, P-804T carbon black and B_4C boron carbide of M20 grade, which ensure the occurrence of exothermic synthesis reactions. Cu powder of PMS-1 grade is the matrix component. The TRC fraction in the initial powder mixture was 23 wt. %. The mixture of powders was thoroughly stirred and poured into a pipe container made of St3 low-carbon structural steel. Primary compaction of the powder mixture was carried out using special equipment. Then the blank was placed in an electric furnace, and heated to the temperature when exothermic reactions began (about 1000 °C). After SHS completion, the hot blank was transferred to a hydraulic press and deformed with a load of at least 250 MPa to eliminate internal porosity. As a result, sandwich plates were obtained, the appearance of which is shown in Fig. 1.

The structure of the composites was studied using a TESCAN VEGAII XMU scanning electron microscope. Rockwell hardness was measured using a hardness tester. The local chemical composition of the composite phases was determined using an OXFORD energy dispersive attachment to a scanning microscope. The average chemical composition of the composites was determined by averaging the scanning results of 10 fragments of the polished section surface with an area of 2×2 mm. Phase X-ray diffraction analysis was performed on a SHIMADZU X-ray diffractometer in chromium k_α-radiation.

Instrumental indentation was carried out on a Fischerscope HM2000 XYm measuring system, using a Vickers indenter and WIN-HCU software at a maximum load of 0.980 N, loading time of 30 s, holding at the load during 50 s and unloading time of 30 s according to ISO 14577 standard. Accuracy of microhardness and microindentation characteristics based on 10 measurements was calculated with a confidence factor of p=0.95.

Based on the indentation results, the following indicators of micromechanical properties were determined: Vickers microhardness (HV), contact elasticity modulus (E^*), elastic recovery index (R_e), component of elastic strain work during indentation (φ), creeping during indentation (C_{IT}), index of elastic deformation fraction in the total deformation during indentation H_{IT}/E (H_{IT} is indentation hardness values at maximum load). The values of the R_e, φ and C_{IT} indicators were calculated using the formulas:

$$R_e = \frac{h_{\max} - h_p}{h_{\max}} \cdot 100\ \%;$$

Fig. 1. *Appearance of sandwich plates made of Cu–Ti–C and Cu–Ti–C–B composites*
Рис. 1. *Внешний вид сэндвич-пластин из композитов Cu–Ti–C и Cu–Ti–C–B*

$$\varphi = \left(1 - \frac{W_e}{W_t}\right) \cdot 100\ \%;$$

$$C_{IT} = \frac{h_{\max} - h_1}{h_1} \cdot 100\ \%,$$

where W_e is the elastic strain work during indentation released when the applied load is removed;
W_t is the total mechanical work during indentation determined by the area under the loading curve;
h_1 is the indenter penetration depth corresponding to the initial point of the horizontal section on the loading curve;
$h_{\max}$ is the maximum penetration depth of the indenter.

Fig. 2 shows the general view of the loading curves and the measured experimental parameters.

RESULTS

Hot pressing of blanks immediately after synthesis completion makes it possible to obtain solid pore-free composites. The average chemical composition of the produced SHS composites is given in Table 1.

According to the results of phase X-ray diffraction analysis, three phases were registered in the Cu–Ti–C composite: a solid solution based on Cu, Cu_4Ti and TiC. TiC particles were formed as a result of an exothermic reaction:

$$Ti + C \rightarrow TiC + Q.$$

Since the SHS process is implemented in air, a carbon combustion reaction occurs in the powder mixture:

$$2C + O_2 \rightarrow 2CO_2 + Q.$$

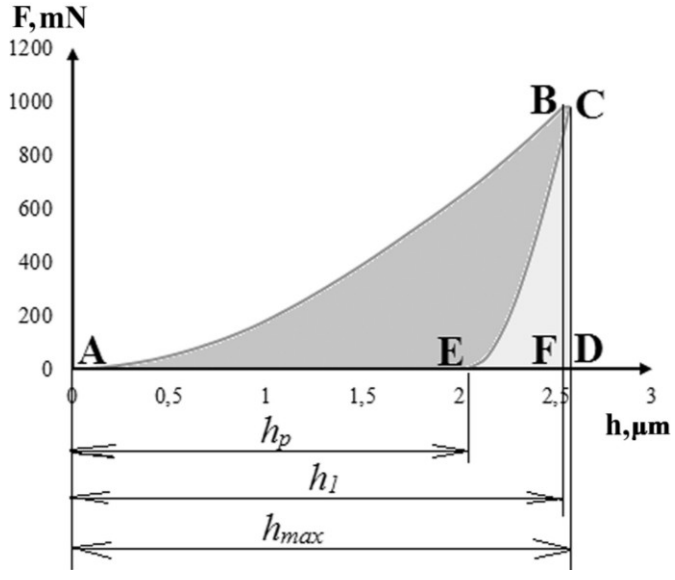

Fig. 2. *Loading diagrams and measured parameters*
Рис. 2. *Диаграммы нагружения и измеряемые параметры*

Phases and chemical elements are distributed nonuniformly over the cross section of the Cu–Ti–C system composite (Fig. 3). Some regions contain a minimal amount of TiC particles (region 1 in Fig. 3 a), while others contain their aggregate (region 2 in Fig. 3 a). Cu_4Ti particles are not visible when examined with a scanning electron microscope due to their small size. When performing a composite EDS analysis, it is impossible to separate phases from each other, so the chemical composition of conventionally identified two structural constituents of the composite was determined: 1 – mechanical mixture of a solid solution based on copper and Cu_4Ti particles with a minimum amount of TiC particles; 2 – Cu+TiC+Cu_4Ti mechanical mixture (Table 2).

The heterogeneity of the distribution of TiC particles throughout the volume of the composite caused the heterogeneity of the distribution of micromechanical properties. In the loading diagrams (Fig. 4 a), the far right curve corresponds to section 1 in Fig. 3 a, and the far left – to section 2 in Fig. 3 a. Consequently, the values of micromechanical properties in Table 3 correspond to the sections indicated in Fig. 3 a. The total hardness of the Cu–Ti–C system composite was 33 HRC.

In the Cu–Ti–C–B system composite, X-ray diffraction analysis, except for the phases found in the Cu–Ti–C composite, additionally detected TiB_2 particles resulting from an exothermic reaction

$$3Ti + B_4C \rightarrow TiC + 2TiB_2 + Q.$$

If TiC particles are uniformly distributed throughout the composite volume, then TiB_2 particles are nonuniformly distributed; there are areas where they are absent. EDS analysis found that TiC particles contain a certain amount of boron (Table 4). It is known that the TiC and TiB compounds are isomorphic, therefore this phase should be designated as Ti(C,B). In the Cu–Ti–C–B composite, two structural components were conventionally identified. Since they differ in chemical composition from the structural constituents of the Cu–Ti–C system composite, letter designations were accepted for them: *A* – Cu+Cu_4Ti+Ti(C,B) mechanical mixture; B – Cu+Cu_4Ti+Ti(C,B)+TiB_2 mechanical mixture (Fig. 5 a). Moreover, particles of unreacted B_4C boron carbide were found in the Cu–Ti–C–B composite (Fig. 5). Thin pure titanium interlayers (marked by arrows in Fig. 5 b) were observed around the B_4C particles.

Since the Cu–Ti–C–B composite additionally contains particles of the strengthening TiB_2 and B_4C phases, its hardness turned out to be slightly higher in comparison to the Cu–Ti–C system composite and amounted to 36 HRC. Micromechanical properties vary throughout the volume of the Cu–Ti–C–B system composite. Compared to the Cu–Ti–C composite, the indicators characterising the strength of the structural components, namely HV, E^*, R_e, H_{IT}/E^*, are higher, and the indicators conditionally characterizing plasticity (h_{max}, φ, C_{IT}) are lower (Table 5).

DISCUSSION

The composites studied in this work differ from those considered previously [19–21] by the lower TRC content in the initial powder mixture. Previously, it was found that the Cu–Ti–C–B system composites retain a certain amount of unreacted B_4C boron carbide. Boron carbide has excessively high hardness and brittleness, and therefore is a source of microcrack initiation under external mechanical loading of parts and structural elements made of this composite during their operation. It turned out that the absence of B_4C particles in the initial powder mixture did not lead to a noticeable decrease in the hardness of the resulting composite. Titanium, which does not participate in exothermic reactions, dissolves in the copper crystal lattice forming a supersaturated solid solution. When cooling the composite in a copper-based solid solution supersaturated with titanium, nano-sized particles of the Cu_4Ti intermetallic compound homogeneously precipitate. These particles significantly strengthen the composite even with a small amount of TiC particles formed and in the absence of TiB_2 particles. The work [18] shows that the Cu–Ti–C system composite has increased resistance to abrasive wear compared to the quench-hardened H12MFL tool die steel, which gives reason to expect high wear resistance of the studied composite.

As shown in [19–21], reducing the TRC proportion in the initial powder mixture for the composite synthesis from 30 wt. % up to 23 wt. % did not affect the retention of unreacted initial B_4C particles in the Cu–Ti–C–B system composite. Obviously, boron carbide particles do not have time to react completely with titanium during the SHS process due to the rapid melting of copper (its melting point is 1083 °C) and the filling of the container mold

Table 1. *Chemical composition of SHS composites*
Таблица 1. *Химический состав СВС-композитов*

System	Units	Ti	C	B	Cu
Cu–Ti–C	Wt. %	23.7±2.3	2.6±0.4	0	The rest
	At. %	26.3±2.1	11.7±1.7	0	
Cu–Ti–C–B	Wt. %	20.4±1.3	3.0±0.4	8.2±1.1	
	At. %	17.0±1.0	9.9±0.9	30.1±3.0	

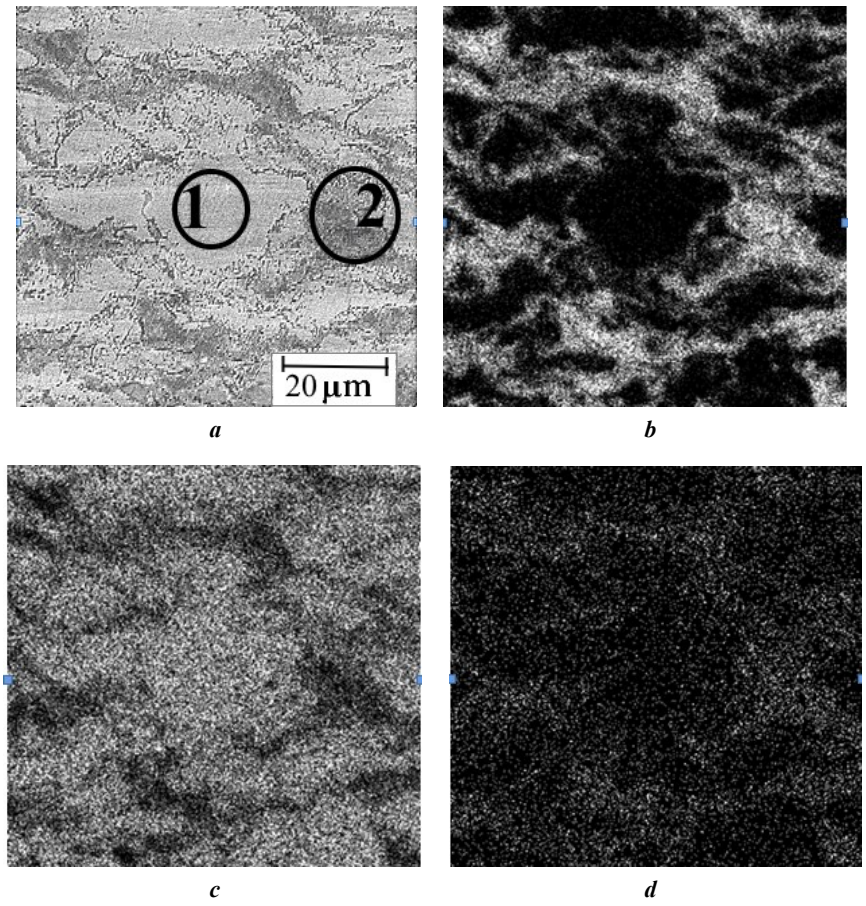

Fig. 3. *Microstructure and pattern of distribution of chemical elements in the Cu–Ti–C system composite:* ***a*** *– secondary electron image;* ***b*** *– characteristic X-rays Ti;* ***c*** *– Cu;* ***d*** *– C*
Рис. 3. *Микроструктура и характер распределения химических элементов в композите системы Cu–Ti–C:* ***a*** *– изображение во вторичных электронах;* ***b*** *– в характеристическом рентгеновском излучении Ti;* ***c*** *– Cu;* ***d*** *– C*

Table 2. *Chemical composition of structural constituents of the Cu–Ti–C system composite, at. % shown in Fig. 3*
Таблица 2. *Химический состав структурных составляющих композита системы Cu–Ti–C, ат. %, представленного на рис. 3*

Structural constituents	C	Ti	Cu	Phases
1	2	22	76	Cu+Cu_4Ti
2	16	52	32	Cu+TiC

Table 3. *Average values of micromechanical properties of structural constituents of the Cu–Ti–C composite*
Таблица 3. *Средние значения микромеханических свойств структурных составляющих композита Cu–Ti–C*

No. in Fig. 3 a	H_{IT}, GPa (±1.5)	HV 0,1 (±1.4)	E^*, GPa (±15)	W_t, nJ (±6.3)	W_e, nJ (±1.2)	h_{max}, µm (±0.2)	h_1, µm (±0.2)	h_p, µm (±0.2)	R_e, %	H_{IT}/E^*	φ, %	C_{IT}, %
1	1.2	116	93	204	20	5.9	5.8	5.0	15	0.013	91	3.4
2	4.9	458	204	105	20	3.1	3.1	2.6	16	0.024	81	1.3

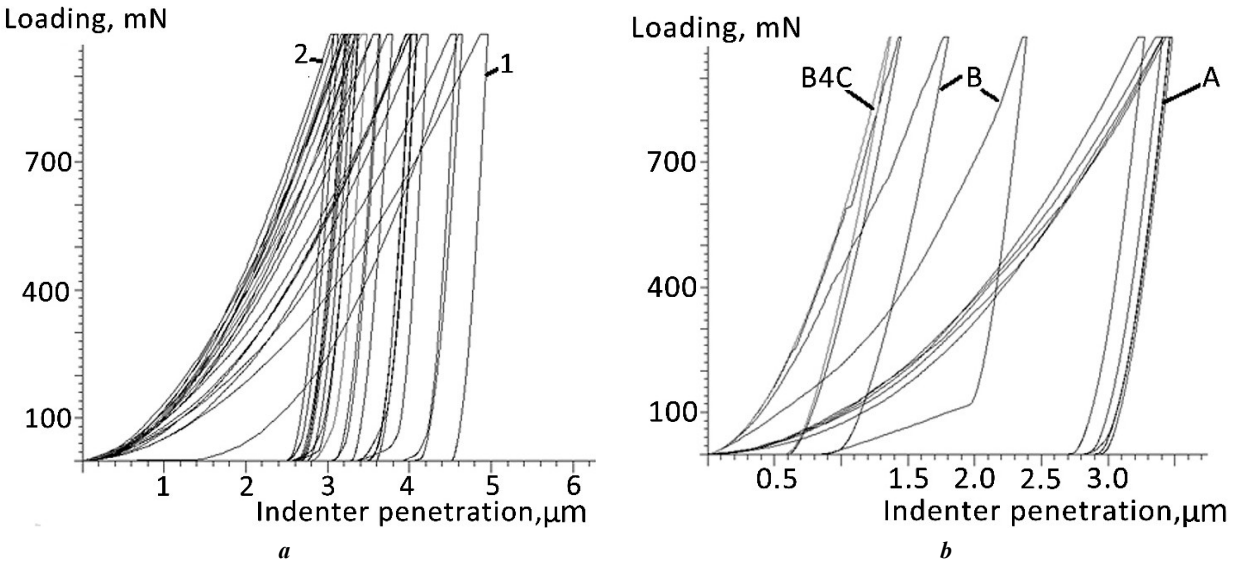

Fig. 4. *Loading diagrams of composites:*
a *– Cu–Ti–C (1 – Cu+Cu$_4$Ti; 2 – Cu+TiC+Cu$_4$Ti);* ***b*** *– Cu–Ti–C–B (A – Cu+Cu$_4$Ti+TiC; B – Cu+TiC+TiB$_2$)*
Рис. 4. *Диаграммы нагружения композитов:*
a *– Cu–Ti–C (1 – Cu+Cu$_4$Ti; 2 – Cu+TiC+Cu$_4$Ti);* ***b*** *– Cu–Ti–C–B (A – Cu+Cu$_4$Ti+TiC; B – Cu+TiC+TiB$_2$)*

Table 4. *Chemical composition of structural constituents of the Cu–Ti–C–B composite, at. % (Fig. 5 a)*
Таблица 4. *Химический состав структурных составляющих композита Cu–Ti–C–B, ат. % (рис. 5 а)*

Structural constituents	B	C	Ti	Cu	Phases
A	8	10	25	58	Cu+Cu$_4$Ti+Ti(C,B)
B	20	11	37	32	Cu+Cu$_4$Ti+Ti(C,B)+TiB$_2$
B$_4$C	70	30	0	0	B$_4$C

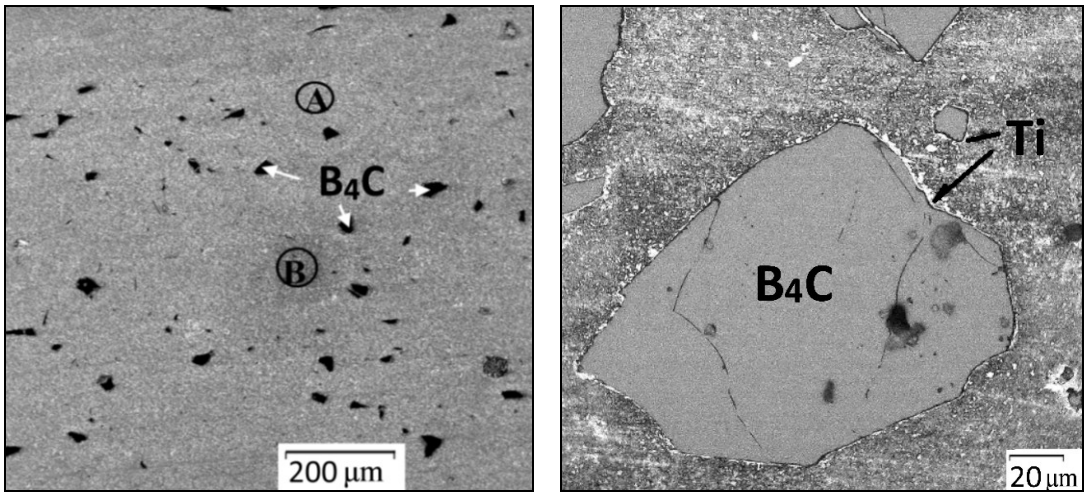

Fig. 5. *Microstructure of the Cu–Ti–C–B system composite:* ***a*** *– magnification ×200;*
b *– magnification ×1000, arrows show titanium interlayers.*
A – Cu+Cu$_4$Ti+Ti(C,B) mechanical mixture; B – Cu+Cu4Ti+Ti(C,B)+TiB$_2$ mechanical mixture
Рис. 5. *Микроструктура композита системы Cu–Ti–C–B:* ***a*** *– увеличение ×200;*
b *– увеличение ×1000, стрелками указаны прослойки титана.*
A – механическая смесь Cu+Cu$_4$Ti+Ti(C,B); B – механическая смесь Cu+Cu$_4$Ti+Ti(C,B)+TiB$_2$

Table 5. *Average values of micromechanical properties of structural constituents of the Cu–Ti–C–B composite (Fig. 5 a)*
Таблица 5. *Средние значения микромеханических свойств структурных составляющих композита Cu–Ti–C–B (рис. 5 а)*

Structural constituents	H_{IT}, GPa (±1.5)	HV 0,1 (±1.4)	E^*, GPa (±15)	W_t, nJ (±6.3)	W_e, nJ (±1.2)	h_{max}, µm (±0.2)	h_1, µm (±0.2)	h_p, µm (±0.2)	R_e, %	H_{IT}/E^*	φ, %	C_{IT}, %
A	3.7	354	180	110	20.0	3.50	3.30	2.90	16	0.021	82	6.0
B	8.3	786	280	80	30.0	2.40	2.30	0.90	64	0.029	63	4.0
B_4C	38.9	3680	283	82	26.2	1.37	1.36	0.58	57	0.093	40	0.7

with the melt. All B_4C particles retained in the composite are surrounded by layers of titanium, which, upon subsequent annealing, is capable of reacting with B_4C particles to form TiB_2 particles, as was shown previously in [21].

The ability to undergo plastic deformation to obtain products of a specified shape is very important for composites. Previously, it was found [20] that plastic deformation of the Cu–Ti–C–B system composites occurs due to the most plastic phases and structural components. From this point of view, the Cu–Ti–C system composite has advantages over the Cu–Ti–C–B system composite, since it contains the Cu+Cu_4Ti structural component with maximum values of the h_{max}, φ and C_{IT} indicators, which characterise the ability to change shape, i. e. to plastic deformation. Since nano-sized particles of the Cu_4Ti intermetallic compound dissolve when heated to temperatures above 700 °C, significant deformation of the Cu–Ti–C system composite should be expected at temperatures of 700–800 °C.

The presence of hard and brittle B_4C particles in the Cu–Ti–C–B system composite reduces its structural strength. Cu+Cu_4Ti+TiC is the most plastic structural constituent in it, which is characterised by higher values of H_{IT}, HV, W_e, R_e, H_{IT}/E^* compared to the Cu+Cu_4Ti constituent in the Cu–Ti–C composite. Nevertheless, plastic deformation of the Cu–Ti–C–B system composite is possible as well under the conditions considered in [20].

The structural constituents of the Cu–Ti–C–B composite are characterised by higher strengthening, which shows a shift of all loading diagrams in the region of smaller indenter penetration depths (Fig. 4), as well as higher values of the H_{IT}, HV, W_e, R_e, H_{IT}/E^* indicators (Table 5). The H_{IT}/E^* ratio determines the proportion of elastic deformation in the total deformation during indentation, and indirectly characterises the wear resistance of the structural components of the composite. For that reason, the Cu–Ti–C–B composite should be expected to demonstrate higher wear resistance compared to the Cu–Ti–C composite, although they practically do not differ in hardness.

CONCLUSIONS

The Cu–Ti–C system composite produced by the SHS method consists of a supersaturated solid titanium solution in a copper crystal lattice, in which nano-sized particles of the Cu_4Ti intermetallic compound homogeneously, precipitated during cooling of the composite are uniformly distributed, and TiC particles formed as a result of the synthesis.

Reducing the TRC proportion in the initial powder mixture from the previously used 30 wt. % up to 23 wt. % did not lead to a decrease in the probability of retaining particles of the original B_4C boron carbide that did not react with the titanium powder through an exothermic reaction.

The most plastic Cu+Cu_4Ti structural component in the Cu–Ti–C composite provides the possibility of subsequent plastic deformation of the composite to obtain a product of a specified shape.

Higher strength indicators of the structural components of the Cu–Ti–C–B system composite determine the expected high wear resistance of products.

REFERENCES

1. Levashov E.A., Rogachev A.S., Kurbatkina V.V., Maksimov Yu.M., Yukhvid V.I. *Perspektivnye materialy i tekhnologii samorasprostranyayushchegosya vysokotemperaturnogo sinteza* [Promissory Materials and Processes of Self-Propagating High-Temperature Synthesis]. Moscow, MISiS Publ., 2011. 378 p.
2. Rogachev A.S., Mukasyan A.S. *Goreniya dlya sinteza materialov* [Combustions for synthesizing materials]. Moscow, FIZMATLIT Publ., 2012. 400 p.
3. Amosov A.P., Borovinskaya I.P., Merzhanov A.G. *Poroshkovaya tekhnologiya samorasprostranyayushchegosya vysokotemperaturnogo sinteza materialov* [Powder technology of self-propagating high-temperature synthesis of materials]. Moscow, Mashinostroenie-1 Publ., 2007. 567 p.
4. Merzhanov A.G. Self-propagating high-temperature synthesis. *Fizicheskaya khimiya. Sovremennye problemy*. Moscow, Khimiya Publ., 1983, pp. 6–44.
5. Latukhin E.I., Umerov E.R., Luts A.R. Self-propagating high-temperature synthesis of porous titanium carbide blanks for subsequent infiltration by melts. *Zagotovitelnye proizvodstva v mashinostroenii*, 2021, vol. 19, no. 7, pp. 322–330. DOI: 10.36652/1684-1107-2021-19-7-322-330.
6. Korosteleva E.N., Korzhova V.V. Structure and phase composition of (TiB)-Ti metal matrix composites obtained by SHS and vacuum sintering. *Russian Physics Journal*, 2020, vol. 63, no. 7, pp. 1195–1201. DOI: 10.1007/s11182-020-02159-4.
7. Sitnikov A.A., Sobachkin A.V., Markov A.M. Peculiarities in formation of different functional coatings of SHS-mechano-composites using technologies of gas-

detonation sputtering. *Naukoemkie tekhnologii v mashinostroenii*, 2020, no. 2, pp. 22–28. DOI: 10.30987/2223-4608-2020-2020-2-22-28.
8. Fedotov A.F., Amosov A.P., Radchenko V.P. *Modelirovanie protsessa pressovaniya poroshkovykh materialov v usloviyakh samorasprostranyayushchegosya vysokotemperaturnogo sinteza* [Modeling the Powder Material Compaction in Conditions of the Self-Propagating High-Temperature Synthesis]. Moscow, Mashinostroenie-1 Publ., 2005. 281 p.
9. Kovalev D.Yu., Bolotskaya A.V., Mikheev M.V. Self-propagating high-temperature synthesis in the Ti–B–Fe system with AlN additions. *Inorganic Materials*, 2022, vol. 58, no. 9, pp. 922–930. EDN: UTUZNA.
10. Krivolutskiy K.S., Amosov A.P., Samboruk A.R. Self-propagating high-temperature sinthesis ultradispersed and nanosized the powder composition TiC–SiC and TiC–NbC. *Vestnik Samarskogo gosudarstvennogo tekhnicheskogo universiteta. Seriya: Tekhnicheskie nauki*, 2016, no. 3, pp. 136–143. EDN: XVSVKB.
11. Shchukin A.S., Sytschev A.E. Peculiarities of a NiAl/Mo transition zone formed during self-propagating high-temperature synthesis. *The Physics of Metals and Metallography*, 2019, vol. 120, no. 9, pp. 848–852. DOI: 10.1134/S0031918X19090138.
12. Lazarev P.A., Busurina M.L., Gryadunov A.N., Sytschev A.E., Boyarchenko O.D., Karpov A.V. structure and phase formation of a Ti–Al–Si based alloy prepared by self-propagating high-temperature synthesis compaction. *Inorganic Materials*, 2022, vol. 58, no. 9, pp. 1005–1010. EDN: QPVISC.
13. Lazarev P.A., Busurina M.L., Sychev A.E. Self-propagating high-temperature synthesis in Ti–Al–Mn. *Fizika goreniya i vzryva*, 2023, vol. 59, no. 1, pp. 85–91. DOI: 10.15372/FGV20230109.
14. Volkov A.Y., Patrakov E.I., Volkova E.G., Komkova D.A., Kalonov A.A., Glukhov A.V., Antonov B.D. Abnormally high strength and low electrical resistivity of the deformed Cu/Mg-composite with a big number of Mg-filaments. *Materials & Design*, 2020, vol. 185, article number 108276. DOI: 10.1016/j.matdes.2019.108276.
15. Kim Ji Soon, Dudina D.V., Kim Jin Chun, Kwon Soon Young, Park Jin Ju, Rhee Chang Kyu. Properties of Cu-based nanocomposites produced by mechanically – activated self – propagating high – temperature synthesis and spark – plasma sintering. *Journal of Nanoscience and Nanotechnology*, 2010, vol. 10, no. 1, pp. 252–257. DOI: 10.1166/jnn.2010.1523.
16. Oanh Nguyen Thi Hoang, Viet Nguyen-Hoang, Kim Ji Soon, Dudina D.V. Structural Investigation of TiC–Cu Nanocomposites Prepared by Ball Milling and Spark Plasma Sintering. *Metals*, 2017, vol. 7, no. 4, article number 123. DOI: 10.3390/met7040123.
17. Volkov A.Yu., Kalonov A.A., Komkova D.A. Effect of annealing on the structure, mechanical and electrical properties of Cu/Mg-composite wires. *Materials Characterization*, 2022, vol. 183, article number 111606. DOI: 10.1016/j.matchar.2021.111606.
18. Tsikarev V.G., Filippenkov A.A., Filippov M.A., Alabushev A.V., Sharapova V.A. Obtaining Ti–Cu–C system composite materials by SHS process. *Izvestiya vysshikh uchebnykh zavedeniy. Poroshkovaya metallurgiya i funktsionalnye pokrytiya*, 2021, vol. 15, no. 4, pp. 4–11. DOI: 10.17073/1997-308X-2021-4-11.
19. Pugacheva N.B., Bykova T.M., Senaeva E.I., Nikolin Y.V. Structure and properties of a SHS Cu–Ti–C–B composite. *The Physics of Metals and Metallography*, 2022, vol. 123, no. 1, pp. 43–49. DOI: 10.1134/S0031918X22010100.
20. Pugacheva N., Kryuchkov D., Bykova T., Vichuzhanin D. Studying the Plastic Deformation of Cu–Ti–C–B Composites in a Favorable Stress State. *Materials*, 2023, vol. 16, no. 8, article number 320. DOI: 10.3390/ma16083204.
21. Pugacheva N.B., Bykova T.M., Senaeva E.I., Goruleva L.S. Thermophysical properties of a Cu–Ti–C–B SHS composite. *Diagnostics, Resource and Mechanics of Materials and Structures*, 2023, no. 3, pp. 50–65. DOI: 10.17804/2410-9908.2023.3.050-065.
22. Nikolin B.V., Matevosyan M.B., Kochugov S.P., Pugacheva N.B. *Sposob izgotovleniya mnogosloynoy iznosostoykoy plastiny* [Method of manufacturing a multilayer wear-resistant plate], patent RF na izobretenie no. 2680489, 2019. 11 p.

СПИСОК ЛИТЕРАТУРЫ

1. Левашов Е.А., Рогачев А.С., Курбаткина В.В., Максимов Ю.М., Юхвид В.И. Перспективные материалы и технологии самораспространяющегося высокотемпературного синтеза. М.: МИСиС, 2011. 378 с.
2. Рогачев А.С., Мукасьян А.С. Горения для синтеза материалов. М.: ФИЗМАТЛИТ, 2012. 400 с.
3. Амосов А.П., Боровинская И.П., Мержанов А.Г. Порошковая технология самораспространяющегося высокотемпературного синтеза материалов. М.: Машиностроение-1, 2007. 567 с.
4. Мержанов А.Г. Самораспространяющийся высокотемпературный синтез // Физическая химия. Современные проблемы. М.: Химия, 1983. С. 6–44.
5. Латухин Е.И., Умеров Э.Р., Луц А.Р. Самораспространяющийся высокотемпературный синтез заготовок пористого карбида титана для последующей инфильтрации расплавами // Заготовительные производства в машиностроении. 2021. Т. 19. № 7. С. 322–330. DOI: 10.36652/1684-1107-2021-19-7-322-330.
6. Коростелева Е.Н., Коржова В.В. Структура и фазовый состав металломатричных композитов (TiB) – Ti, полученных в процессе СВС и вакуумного спекания // Известия вузов. Физика. 2020. Т. 63. № 7. С. 81–87. DOI: 10.17223/00213411/63/7/81.
7. Ситников А.А., Собачкин А.В., Марков А.М. Особенности формирования различных функциональных покрытий из СВС-механокомпозитов с помощью технологии газодетонационного напыления // Наукоемкие технологии в машиностроении. 2020. № 2. С. 22–28. DOI: 10.30987/2223-4608-2020-2020-2-22-28.
8. Федотов А.Ф., Амосов А.П., Радченко В.П. Моделирование процесса прессования порошковых материалов в условиях самораспространяющегося высокотемпературного синтеза. М.: Машиностроение-1, 2005. 281 с.
9. Ковалев Д.Ю., Болоцкая А.В., Михеев М.В. Самораспространяющийся высокотемпературный синтез

в системе Ti–B–Fe с добавкой AlN // Неорганические материалы. 2022. Т. 58. № 9. С. 956–964. EDN: TJQGMZ.
10. Криволуцкий К.С., Амосов А.П., Самборук А.Р. Самораспространяющийся высокотемпературный синтез ультрадисперсных и наноразмерных порошков композиций TiC–SiC и TiC–NbC // Вестник Самарского государственного технического университета. Серия: Технические науки. 2016. № 3. С. 136–143. EDN: XVSVKB.
11. Щукин А.С., Сычёв А.Е. Особенности строения переходной зоны NiAl/Mo, сформированной в процессе самораспространяющегося высокотемпературного синтеза // Физика металлов и металловедения. 2019. Т. 120. № 9. С. 925–930. DOI: 10.1134/S0015323019090134.
12. Лазарев П.А., Бусурина М.Л., Грядунов А.Н., Сычев А.Е., Боярченко О.Д., Карпов А.В. Особенности структуры и фазообразования сплава на основе Ti–Al–Si, полученного методом СВС-компактирования // Неорганические материалы. 2022. Т. 58. № 9. С. 1039–1044. EDN: XTLFSK.
13. Лазарев П.А., Бусурина М.Л., Сычёв А.Е. Самораспространяющийся высокотемпературный синтез в системе Ti–Al–Mn // Физика горения и взрыва. 2023. Т. 59. № 1. С. 85–91. DOI: 10.15372/FGV20230109.
14. Volkov A.Y., Patrakov E.I., Volkova E.G., Komkova D.A., Kalonov A.A., Glukhov A.V., Antonov B.D. Abnormally high strength and low electrical resistivity of the deformed Cu/Mg-composite with a big number of Mg-filaments // Materials & Design. 2020. Vol. 185. Article number 108276. DOI: 10.1016/j.matdes.2019.108276.
15. Kim Ji Soon, Dudina D.V., Kim Jin Chun, Kwon Soon Young, Park Jin Ju, Rhee Chang Kyu. Properties of Cu-based nanocomposites produced by mechanically – activated self – propagating high – temperature synthesis and spark – plasma sintering // Journal of Nanoscience and Nanotechnology. 2010. Vol. 10. № 1. P. 252–257. DOI: 10.1166/jnn.2010.1523.
16. Oanh Nguyen Thi Hoang, Viet Nguyen-Hoang, Kim Ji Soon, Dudina D.V. Structural Investigation of TiC–Cu Nanocomposites Prepared by Ball Milling and Spark Plasma Sintering // Metals. 2017. Vol. 7. № 4. Article number 123. DOI: 10.3390/met7040123.
17. Volkov A.Yu., Kalonov A.A., Komkova D.A. Effect of annealing on the structure, mechanical and electrical properties of Cu/Mg-composite wires // Materials Characterization. 2022. Vol. 183. Article number 111606. DOI: 10.1016/j.matchar.2021.111606.
18. Цикарев В.Г., Филиппенков А.А., Филиппов М.А., Алабушев А.В., Шарапова В.А. Опыт получения композиционных материалов системы Ti–Cu–C СВС-процессом // Известия высших учебных заведений. Порошковая металлургия и функциональные покрытия. 2021. Т. 15. № 4. С. 4–11. DOI: 10.17073/1997-308X-2021-4-11.
19. Пугачева Н.Б., Николин Ю.В., Быкова Т.М., Сенаева Е.И. Структура и свойства СВС-композита системы Cu–Ti–C–B // Физика металлов и металловедение. 2022. Т. 123. № 1. С. 47–54. DOI: 10.31857/S0015323022010107.
20. Pugacheva N., Kryuchkov D., Bykova T., Vichuzhanin D. Studying the Plastic Deformation of Cu–Ti–C–B Composites in a Favorable Stress State // Materials. 2023. Vol. 16. № 8. Article number 320. DOI: 10.3390/ma16083204.
21. Пугачева Н.Б., Быкова Т.М., Сенаева Е.И., Горулёва Л.С. Теплофизические свойства СВС композитов Cu–Ti–C–B // Diagnostics, Resource and Mechanics of Materials and Structures. 2023. № 3. С. 50–65. DOI: 10.17804/2410-9908.2023.3.050-065.
22. Николин Б.В., Матевосян М.Б., Кочугов С.П., Пугачева Н.Б. Способ изготовления многослойной износостойкой пластины: патент РФ на изобретение № 2680489, 2019. 11 с.

Структура и микромеханические свойства СВС-композитов с медной матрицей: особенности формирования

Пугачева Наталия Борисовна[1], доктор технических наук, доцент, главный научный сотрудник
Быкова Татьяна Михайловна*[2], кандидат технических наук, старший научный сотрудник
Сенаева Екатерина Игоревна[3], младший научный сотрудник
Институт машиноведения имени Э.С. Горкунова Уральского отделения РАН, Екатеринбург (Россия)

***E-mail: nat@imach.uran.ru, tatiana_8801@mail.ru**

[1]ORCID: https://orcid.org/0000-0001-8015-8120
[2]ORCID: https://orcid.org/0000-0002-8888-6410
[3]ORCID: https://orcid.org/0000-0001-8625-2310

Поступила в редакцию 22.06.2023 *Принята к публикации 19.10.2023*

Аннотация: Самораспространяющийся высокотемпературный синтез (СВС) является одним из перспективных способов получения прочных и износостойких композитов. Особый интерес представляет использование меди в качестве матрицы из-за уникального сочетания электро- и теплопроводности. Монолитные СВС-композиты системы Cu–Ti–C–B и Cu–Ti–C в настоящее время мало изучены. Сведения о фазовом составе таких композитов весьма противоречивы, а данные по микромеханическим свойствам практически отсутствуют. В работе представлены результаты сравнительного анализа структуры и микромеханических свойств композитов систем Cu–Ti–C

и Cu–Ti–C–B. Установлено, что матрицей обоих композитов является пересыщенный титаном твердый раствор на основе меди, в котором при охлаждении выделяются наноразмерные частицы интерметаллида Cu_4Ti. Упрочняющими фазами, образующимися в результате СВС, являются частицы TiC (композит Cu–Ti–C) и частицы TiC и TiB_2 (композит Cu–Ti–C–B). В композите Cu–Ti–C–B сохранились исходные частицы непрореагировавшего карбида бора B_4C, микротвердость которых составила 3680 *HV* 0,1. Наиболее пластичной структурной составляющей является механическая смесь $Cu+Cu_4Ti$ в композите системы Cu–Ti–B, за счет которой возможна последующая пластическая деформация с целью получения деталей заданной формы. При исследовании микромеханических свойств максимальные показатели прочности H_{IT}, HV, W_e, R_e, H_{IT}/E^* были зафиксированы в композите системы Cu–Ti–C–B, что позволяет ожидать высокую износостойкость изделий из него.

Ключевые слова: самораспространяющийся высокотемпературный синтез; монолитные СВС-композиты; медная матрица; структурные составляющие; упрочняющие фазы; интерметаллиды; карбид титана; диборид титана; микромеханические свойства; твердость.

Благодарности: Исследования выполнены за счет гранта РНФ № 22-29-00188 «Разработка научных и технологических основ формирования монолитных СВС-композитов системы Cu–Ti–C–B с заданными функциональными свойствами», https://rscf.ru/project/22-29-00188/.

Работа выполнена на оборудовании Центра коллективного пользования «Пластометрия» федерального государственного бюджетного учреждения науки Института машиноведения имени Э.С. Горкунова Уральского отделения Российской академии наук.

Статья подготовлена по материалам докладов участников XI Международной школы «Физическое материаловедение» (ШФМ-2023), Тольятти, 11–15 сентября 2023 года.

Для цитирования: Пугачева Н.Б., Быкова Т.М., Сенаева Е.И. Структура и микромеханические свойства СВС-композитов с медной матрицей: особенности формирования // Frontier Materials & Technologies. 2023. № 4. С. 99–108. DOI: 10.18323/2782-4039-2023-4-66-9.